

## TWO METHODS FOR DETERMINATION OF THE EFFECTIVE WAVENUMBER OF GAUSSIAN BEAMS IN ABSOLUTE GRAVIMETERS

Petr Křen<sup>1)</sup>, Vojtech Pálinkás<sup>2)</sup>

1) Czech Metrology Institute, Okružní 31, 63800 Brno, Czech Republic (✉ [pkren@cmi.cz](mailto:pkren@cmi.cz), +420 257 288 388).

2) Research Institute of Geodesy, Topography and Cartography, Geodetic Observatory Pecny, 25165 Ondřejov 244, Czech Republic ([vojtech.palinkas@pecny.cz](mailto:vojtech.palinkas@pecny.cz))

### Abstract

This paper presents two methods for evaluation of the effective wavenumber of nearly-Gaussian beams in laser interferometers that can be used for determination of a so called diffraction correction in absolute gravimeters. The first method, that can be simply used in situ, is an empirical procedure based on the evaluation of the variability of  $g$  measurements against the amount of light limited by an iris diaphragm and transmitted to a photodetector. However, precision of this method depends on the beam quality similarly as in the case of the conventional method based on measurement of a beam width. The second method, that is more complex, is based on beam profiling in various distances and on calculation of the effective wavenumber using the second spatial derivative of a non-ideal beam field envelope. The measurement results achieved by both methods are presented on an example of two absolute gravimeters and the determined diffraction corrections are compared with the results obtained by measurements of beam width. Agreement of methods within about  $1 \mu\text{Gal}$  have been obtained with average diffraction corrections slightly exceeding  $+2 \mu\text{Gal}$  for three FG5(X) gravimeter configurations.

Keywords: diffraction correction, effective wavenumber, interferometer, Gaussian beam, absolute gravimeter.

© 2018 Polish Academy of Sciences. All rights reserved

### 1. Introduction

The diffraction effect of laser beams used in optical interferometers has to be taken into account in high-accurate distance measurements. The corresponding correction, expressed as the determination of the effective wavelength or wavenumber, was studied by Monchalin *et al.* in [1] and by Sasso *et al.* in [2]. Absolute gravimeters with macroscopic masses employ a modified Mach-Zehnder laser interferometer to measure the distance of a free-falling test mass in vacuum [3]. The effect of diffraction in absolute gravimeters was estimated in [4, 5], the beam waist approximation being consistent with [1]. Nevertheless, the real waist of laser beams of absolute gravimeters is only rarely determined or it is approximated by a beam width at a particular distance. For the most accurate type of gravimeters (FG5 and FG5X), for which a standard uncertainty of  $2\text{--}3 \mu\text{Gal}$  ( $1 \mu\text{Gal} = 10 \text{ nm/s}^2$ , *i.e.*  $\approx 10^{-9}$  relative in acceleration or displacement) is declared, the diffraction correction of  $1.2 \mu\text{Gal}$  is usually applied, as shown in [6]. Moreover,

according to [2], the wavefront perturbations and deviations from a fundamental-mode Gaussian intensity-profile have to be taken into account at a relative accuracy level of  $10^{-9}$ . To our knowledge, such an approach has never been applied to absolute gravimeters and diffraction corrections are computed based on the beam width measurement [4, 5] at one selected distance and referred to as a beam waist [4].

In this paper, we present two methods for the determination of the effective wavenumber and related diffraction correction: 1) an approximate method for fundamental-mode Gaussian beams based on an *in situ* experiment that does not require the direct measurement of the beam waist size of nearly collimated coaxial beams and 2) a general method using camera-based beam profiling that takes into account non-ideal Gaussian beams.

Further, we will show that a beam quality ( $M^2$ ) factor is an important parameter for the FG5(X) gravimeters. The knowledge of laser beam parameters influences the accuracy of present gravimeters, both working with a macroscopic object or cold atoms [7], thus contributing to the accuracy of new SI realization of kilogram with a Kibble balance. A new SI realization of mole via the Si lattice parameter also needs to carefully take into account a “diffraction correction” of beams used in interferometers [8]. Moreover, the volume determination of silicon spheres also deals with the Gouy shift and the “diffraction effect”, both related to a change of effective wavenumber. It has the main contribution to the uncertainty of measurement [9], similarly as in the new alternative realization of kilogram with the XRCD method [10]. For example, in the case of a uniform beam profile the total Gouy shift varies from  $-\pi$  up to  $-2\pi$  [11] (compare with  $-\pi$  for a fundamental-mode Gaussian beam with  $M^2 = 1$ ). It is known that the pure higher-order Hermite-Gaussian or Laguerre-Gaussian beam modes have the Gouy shift multiplied by an integer [1] that equals to their  $M^2$  factor. Thus, it can be assumed that from the modal decomposition of an arbitrary beam there will be a factor  $F$  (generally not an integer) that will modify the Gouy shift effect in real beams. Consequently, if the measured beam quality is  $M^2 = 1.2$ , as in [12], the phase correction will be underestimated in the volume determination of silicon sphere. Generally, we can see that optical beams play a significant role in future realizations of SI and that a correct treatment of the diffraction effects including the beam quality has to be carefully investigated.

## 2. Method with iris diaphragm

In the Monchalin’s approach [1] (11), the beam widths  $w_1$  and  $w_2$  of the collimated reference and measuring beams are approximated by the beam waist  $w_0$ . The effective wavenumber  $\bar{k}$  (in  $z$  direction) within aperture of radius  $\rho$  is given by:

$$\bar{k}(\rho) = k \left[ 1 - \left( \frac{\lambda}{2\pi w_0} \right)^2 \left( 1 + \frac{2\rho^2 w_0^{-2}}{\exp(2\rho^2 w_0^{-2} - 1)} \right) \right], \quad (1)$$

where  $k$  is the wavenumber related to the vacuum wavelength as  $k = 2\pi/\lambda$ . Note that without aperture (as  $\rho$  tends to infinity) the second term in round brackets is equal to 1 and (1) becomes identical with (12) in [1]. Further we would like to point out that the symbol overline will be used in this paper to demonstrate the character of averaging (over the beam within a given radius).

The optical power of fundamental Gaussian beams encircled within a radius  $\rho$  is:

$$\bar{P}(\rho) = \bar{P}(\infty) (1 - \exp(-2\rho^2 w_0^{-2})). \quad (2)$$

If the aperture is limited by an iris diaphragm and the relative interference power  $\bar{x}(\rho) = \bar{P}(\rho)/\bar{P}(\infty)$  is determined from the fringe signal amplitudes, then the effective wavenumber from (1) might be expressed, substituting  $2\rho^2 w_0^{-2} = -\ln(1 - \bar{x})$  obtained from (2), as a linear function of dimensionless factor:

$$f(\bar{x}) = (\bar{x}^{-1} - 1) \ln(1 - \bar{x}) - 1, \quad (3)$$

and therefore also measurements of  $g$ , that linearly depend on the distance measurements, can be determined as:

$$g(\bar{x}) = g_{correct} + s f(\bar{x}), \quad (4)$$

where  $g_{correct}$  is the  $g$ -value that corresponds to the vacuum wavelength  $\lambda$  determined by the optical frequency calibration and the second term represents the diffraction effect. Since  $f(\bar{x}) = -1$  for a beam without limitation by a diaphragm, the slope  $s$  corresponds to the diffraction correction. In principle, only two measurements ( $g$ -values, in our case) are necessary for the experimental determination of  $s$ , the first with the fully opened iris diaphragm and the second with a partly closed diaphragm. Besides,  $\bar{x}$  has to be determined but there is no need to know  $\rho$  and  $w_0$ .

We have to point out that the described method is valid only for the fundamental-mode Gaussian beams ( $M^2 = 1$ ). It means that it has principally the same limitations as the usual method where the beam waist is determined by a knife-edge beam blocking [4]. An advantage of the discussed method is that the diffraction correction is determined within the gravimeter itself (*i.e.* applied approximately at a correct distance), the only necessity is to attach the iris diaphragm in front of the detector (see Fig. 1). Therefore, it is easy to repeat a measurement and the real effect on  $g$  is observed (instead of a blind correction) for nearly-ideal beams. However, it is clear that the drop-to-drop scatter of  $g$  measurements contributes to the evaluation uncertainty of the diffraction correction.

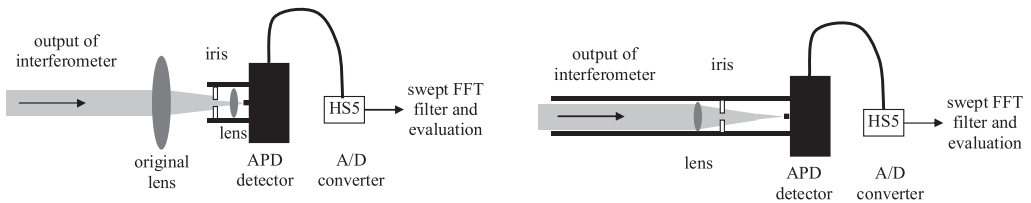


Fig. 1. A measurement scheme of modified absolute gravimeters FG5 and FG5X equipped with a convex lens, an iris diaphragm (within a tube mounted to the threads of the detector), APD and an HS5 system [13].

To verify the method experimentally, the detection system of fringe signals in absolute gravimeters FG5-215 and FG5X-251 were modified according to [13, 14]. Further, we used a fast avalanche photodiode (APD, Thorlabs APD430A/M) with centred mounting of a convex lens and an iris diaphragm for modifications of  $\bar{x}$ . FG5X-251 gravimeter has been tested in two configurations, the first one with the original input beam collimator and the second one with the new triplet collimator (Thorlabs TC25APC-633) (the reason for using different collimators will be explained below).

The measurement results related to FG5-215 are illustrated in Fig. 2 and approximated by a single regression line with a slope that also represents (according to (4)) the measured diffraction effect. Its value (with reference to a beam with infinite width) and standard deviation estimated from data obtained during three non-consecutive measurement days are  $(-1.71 \pm 0.53) \mu\text{Gal}$  and correspond approximately to a relative error of about  $1.7 \cdot 10^{-9}$  of the displacement measurement.

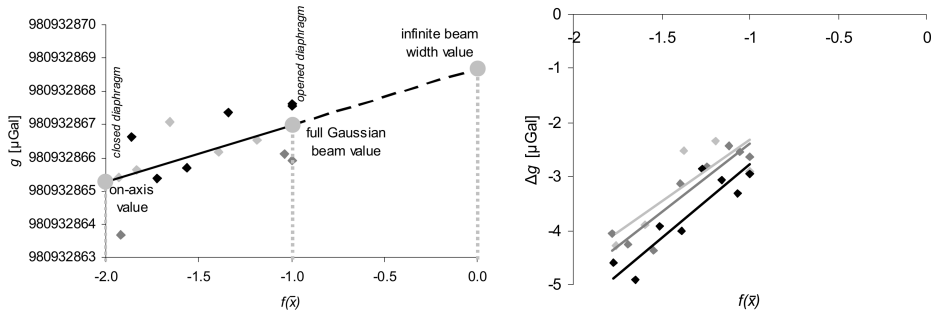


Fig. 2. Left: The absolute gravity acceleration  $g$  measured by gravimeter FG5-215 as a function of a dimensionless parameter  $f(\bar{x})$ , given by (3), that depends on the interference power limited by the iris diaphragm. All  $g$ -values (diamonds) represent averages from about 300 drops and were obtained from three non-consecutive measurement days (in Feb. and Mar. 2017). Three grey circles represent  $g$ -values in illustrative cases for a given linear fit. Right: the  $g$ -differences between two measurement systems of gravimeter FG5X-251 achieved for a setup with the original collimator (measured in Aug. 2017). Interferometer alignments are shown distinguished by the lightness of symbols. Note that displayed are differences of  $g$ -values obtained from the complementary output with reference to the original output systems and thus the correct extrapolation does not intersect zero difference at  $f(\bar{x}) = 0$ .

In the case of FG5X-251, two detection systems were running in parallel during the experiments with the iris diaphragm. The original system was kept without any change and the iris diaphragm was mounted to a new HS5 system (analogue-to-digital converter TiePie Handyscope HS5-530XMS with a swept FFT filter, see [13, 14]). A huge advantage of the two parallel measurement systems is that the  $g$ -values determined from the same free falls contain similar noise contributions which are suppressed in  $g$ -differences. A low noise level in  $g$ -differences (about  $1 \mu\text{Gal}$  for one free-fall) enables a more effective examination of the effects influencing one of the two systems. The  $g$ -differences between both systems related to variable openings of the iris diaphragm were measured for two configurations of FG5X-251, the first one with the original input beam collimator (see Fig. 2) and the second one with the new triplet collimator. The diffraction effects with error estimates were obtained as an average and standard deviation of three slopes reaching  $(-2.51 \pm 0.20) \mu\text{Gal}$  and  $(-1.78 \pm 0.24) \mu\text{Gal}$  for the original and new collimators, respectively.

### 3. Method with profiling camera

The second, more complex and general method for the determination of the diffraction correction is based on the beam profiling using a digital camera with calibrated pixel spacing. It enables to determine parameters of non-ideal Gaussian beams in the interferometer and thus the effective wavenumber.

#### 3.1. Beam parameters

Evolution of beam width  $w$  along the direction of propagation was determined for gravimeters FG5-215 and FG5X-251 (in two configurations, with the original and Thorlabs triplet collimators) by analyzing beam profiles at different distances measured at the outputs of gravimeters. The first two examples are shown in Fig. 3. The expected evolution of a Gaussian beam width along the  $z$ -axis is given by:

$$w^2(z) = w_0^2 \left( z_R^2 + (z - z_0)^2 \right) z_R^{-2}, \quad (5)$$

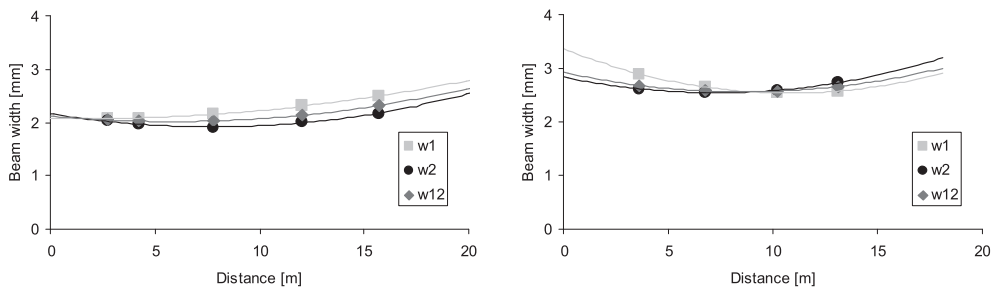


Fig. 3. Evolution of beam widths  $w$  obtained from the second moment beam width ( $D4\sigma$ ) for the reference beam  $w_1$ , measuring beam  $w_2$  and their combination  $w_{12}$  determined by the profiling camera at several distances for outputs of FG5 gravimeter (without fibre optics with  $5\times$  beam expander directly from an He-Ne laser) and FG5X gravimeter with the original collimator.

where three parameters – the Rayleigh length  $z_R$ , the beam waist position  $z_0$  and  $w_0$  together with the derived beam quality ( $M^2$ ) factor describe the beam according to the ISO standard 11146. The results for three beams related to three gravimeter setups are shown in Table 1. We can see that the original fibre collimator of FG5X-251 gravimeter significantly deteriorates the beam quality, which can also be clearly seen from the beam profiles at larger distances (see Fig. 4).

Table 1. Parameters of the measuring beams in gravimeters. The “expected” Rayleigh length is related to a single determination of the beam width close to the gravimeter with assumed  $M^2 = 1$ . The “measured” Rayleigh lengths were determined from the evolution of the beam width along the direction of beam propagation, the beam widths have to be determined for at least three distances to evaluate three beam parameters including the beam quality factor  $M^2$  or the beam waist. The accuracy of beam waist estimation, expressed from the error of fitting parameters given by (5), is below 0.05 mm.

configuration	Rayleigh length		$M^2$	waist [mm]
	expected [m]	measured [m]		
FG5 with original expander	20.3	14.8	1.23	1.91
FG5X with original collimator	34.0	14.9	2.16	2.54
FG5X with new triplet collimator	23.3	17.3	1.22	2.06

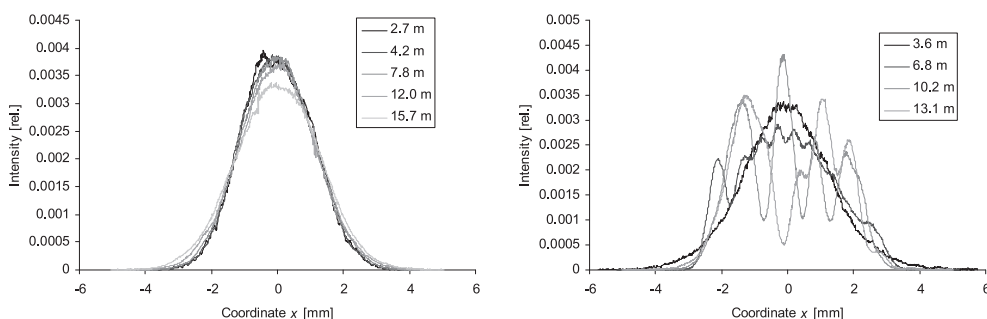


Fig. 4. Beam profiles of the reference beams measured at several distances (the same as in Fig. 3; the curve lightness is increasing with distance indicated in legend) from outputs of the gravimeters FG5-215 (left) and FG5X-251 with the original collimator (right).

Note, that the diffraction correction given by Monchalin’s approach is computed from the beam waist. However, the position of the beam waist is often far outside (5–10 m) the gravimeters, as it can be seen in Fig. 3. Thus, the evaluation from a beam width at one position (*e.g.* inside or close to the gravimeter) always underestimates the diffraction effect according to [1]. For example, in the case of FG5-215, the beam waist is 1.91 mm and beam width in the gravimeter is of about 2.2 mm that leads to corrections of 2.72  $\mu\text{Gal}$  and 2.1  $\mu\text{Gal}$ , respectively.

### 3.2. Determination of effective wavenumber

The propagation of a complex amplitude  $E$  of the beam envelope in the paraxial approximation is given by the Helmholtz equation:

$$\left( \nabla_{\perp}^2 - 2ik \frac{\partial}{\partial z} \right) E(x, y, z) = 0, \tag{6}$$

where:

$$\nabla_{\perp}^2 = \frac{\partial^2}{\partial x^2} + \frac{\partial^2}{\partial y^2} \tag{7}$$

is the transverse part of the Laplacian. The wavenumber in  $z$  direction is given in the paraxial approximation as:

$$k_z = k \sqrt{1 - \frac{k_x^2 + k_y^2}{k^2}} \cong k - \frac{k_x^2 + k_y^2}{2k}. \tag{8}$$

It is known from Fourier optics that the wavenumber components correspond to partial derivatives in direct space. Then, we could calculate the deviation of the effective wavenumber in  $z$  direction approximately as:

$$\kappa(x, y, z) \cong \text{Re} \left\{ \frac{\nabla_{\perp}^2 E(x, y, z)}{2kE(x, y, z)} \right\}. \tag{9}$$

The fundamental Gaussian mode of the electric field could be written as:

$$E(x, y, z) = E(0, 0, z) \exp\left(-\frac{r^2}{w^2}\right) \exp\left(-ik \frac{r^2}{2R}\right), \tag{10}$$

where  $z = 0$  corresponds to the position of beam waist  $w_0$ , the beam width  $w$  is given by the relation (5) and the radius of curvature  $R$  is:

$$R(z) = (z_R^2 + z^2) z^{-1}. \tag{11}$$

The first exponential term of (10) can be named a diffraction term and the second exponential term – a divergence term.

Since in our experiments with a digital camera (without a wavefront sensor) we were able to determine only intensity beam profiles  $I$ , we can calculate  $E$  simply as  $E_{diff}$ :

$$E_{diff}(x, y, z) = \sqrt{I(x, y, z)}. \tag{12}$$

However, we cannot resolve the divergence term that should be included. In the paraxial approximation, we can suppose that the radius of curvature is a function of  $z$  only:

$$R(x, y, z) = R(z). \tag{13}$$

The experimental results in Fig. 3 show that the evolution of beam width  $w$  can be well represented by the relation (5). Thus, we could expect  $R$  as a function of  $z$  relative to the position of beam waist  $z_0$ :

$$\frac{1}{R^2(z)} = \frac{(z - z_0)^2}{(z_R^2 + (z - z_0)^2)^2}. \quad (14)$$

If we include the divergence term (as a radial phase dependency) to our evaluation of field  $E$  from camera images, we obtain:

$$E(x, y, z) = \sqrt{I(x, y, z)} \exp\left(-ik \frac{r^2}{2R(z)}\right) \quad (15)$$

and further from (9) we will obtain the total evaluation of the effective wavenumber deviation in the form

$$\kappa_{tot}(x, y, z) = \kappa_{diff}(x, y, z) - k \frac{r^2}{2R^2(z)}, \quad (16)$$

where the first term is the diffraction term (representing the second derivatives from (9) for a field given by (12) without a divergence term) and the second term corresponds to the divergence term (local cosine error).

Electric fields of the reference beam  $E_1$  and the measuring beam  $E_2$  interfere on the detector. The reference beam, which propagates through the static arm of interferometer, works as a soft-aperture in paraxial approximation. The effective wavenumber must be evaluated from the measuring beam using (16) and weighted by the interference field, because only interference fringes represent the detected signal of interferometer. The origin of  $x$  and  $y$  coordinates is evaluated from the centroid of interfering fields. Then, the effective wavenumber deviation for the diffractive term  $\kappa_{diff}$  over the full beam can be expressed as:

$$\bar{\kappa}_{diff}(z) \cong \frac{\iint \kappa_{diff}(x, y, z) E_1 E_2 dx dy}{\iint E_1 E_2 dx dy} \cong \frac{1}{2k} \frac{\iint \left( \sqrt{I_1(x, y, z)} \nabla_{\perp}^2 \sqrt{I_2(x, y, z)} \right) dx dy}{\iint \sqrt{I_1(x, y, z)} \sqrt{I_2(x, y, z)} dx dy}, \quad (17)$$

where the integrations (or corresponding summations) are performed over the area of camera that covers most of the beam power. To suppress the effect of image-clipping, the half-size of the integration area given by the window size has been chosen as the beam width multiplied by a fixed factor of 2 (*i.e.*  $D4\sigma$ -sized for Gaussian beams). It is close to the optimal values obtained in [15] for a minimal sensitivity to the camera background. The total effective wavenumber deviation over the full beam, including the divergence term, can be calculated as:

$$\bar{\kappa}_{tot}(z) = \bar{\kappa}_{diff}(z) - \frac{k w_{12}^2}{4R^2(z)}, \quad (18)$$

where the width  $w_{12}$  is obtained from both beams (reference beam 1 and measuring beam 2) as:

$$\frac{w_{12}^2}{2} = \frac{\iint r^2 E_1 E_2 dx dy}{\iint E_1 E_2 dx dy}. \quad (19)$$

Let us also note that the total phase shift of an interferometer between the points given by the positions  $z_A$  and  $z_B$  is given by:

$$\varphi = \int_{z_A}^{z_B} \bar{\kappa}(z) dz. \quad (20)$$

In the case of gravimeters, where the displacement is relatively small (a few decimetres) with reference to the Rayleigh length, we can directly use the local effective wavenumber from (18).

### 3.3. Evaluation of camera images

The second derivatives of the electric field for each point (a pixel of camera images) of the measuring beam in (17) were evaluated through fitting the field  $E_2$  by a fourth order 2D polynomial on coordinate differences from pixel coordinates  $x$  and  $y$  (i.e. moving least squares with unit weight in a given moving area, see Fig. 5):

$$E_2(x' - x, y' - y) = \sum_{i+j \leq 4} E_{2ij}(x, y) (x' - x)^i (y' - y)^j. \quad (21)$$

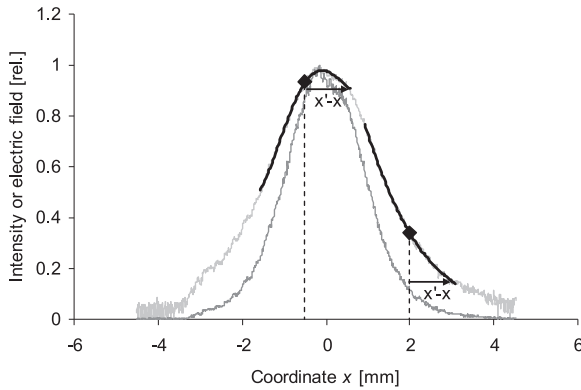


Fig. 5. An example of the intensity beam profile (dark grey) and its square root, i.e. electric field (light grey). Two local fourth order fits (black lines) at two points are shown in 1D. The second order coefficients of corresponding fits in 2D were used for the evaluation of the second derivatives according to (22).

The fits were carried out on a data range given by the size of approximately the width  $w_2$  to avoid large local derivatives of the beam profile due to the measurement noise. These ranges were selected symmetrically around each point and thus we can directly write:

$$\nabla_{\perp}^2 E_2(x, y) = 2(E_{220}(x, y) + E_{202}(x, y)), \quad (22)$$

because the second order coefficients of the polynomial in  $x$  or  $y$  correspond to the second derivatives of Taylor series around this point.

The local fitting by the fourth order polynomial was also applied to the intensity profile  $I_b$  of a beam  $b$  since it helps to improve the performance of beam width estimation that depends on the correct background subtraction. The range of the intensity local fits should be smaller than for the electric field. The resulting coefficients  $I_{b00}(x, y)$  with indices  $i = 0$  and  $j = 0$  correspond to a smoothed profile of the intensity. The minimal value of  $I_{b00}$  within the range of beam width estimation was used for subtracting the camera electrical and optical backgrounds. Such a smoothing is advantageous, because it removes a bias of evaluated electric field  $E$  (that is in principle also negative and we determine it as a positive square root of  $I$ ) caused by the camera noise affecting directly intensity  $I$ . We verified the effect of background and noise on the evaluation of images by setting different exposition times and we found a negligible effect on the determination of the diffraction correction. It represents a successful test of parasitic effects caused by the non-linearity of camera pixel readings.

### 3.4. Results of method

The Monchalin's approximation (given by (12) in [1]) is exactly valid only at the position of beam waist for the fundamental Gaussian mode. We could simply calculate that as beam spreads at larger distances from the beam waist, the Monchalin's approximation (where the beam width is approximated by the beam waist) cannot be used outside the Rayleigh range and it tends to zero effects at infinite distance, if a single locally evaluated width is used to determine the correction. Thus, the divergence effect should be also taken into account. From Fig. 6 we can see that the diffractive term obtained from the second derivatives of beam profiles is almost identical with Monchalin's approximation for high quality beams with  $M^2$  close to 1 (FG5X with the triplet collimator). On the other hand, if the beam quality decreases (FG5X with the original collimator), the difference between the two evaluations becomes significant. Further, it can be seen that the divergence terms are smaller than the diffractive terms that represent the diffraction effect of a plane wave-front limited by the finite beam profile. It shows that the beam divergences are too small to be measured correctly by a compact wavefront sensor in the case of FG5(X) gravimeters.

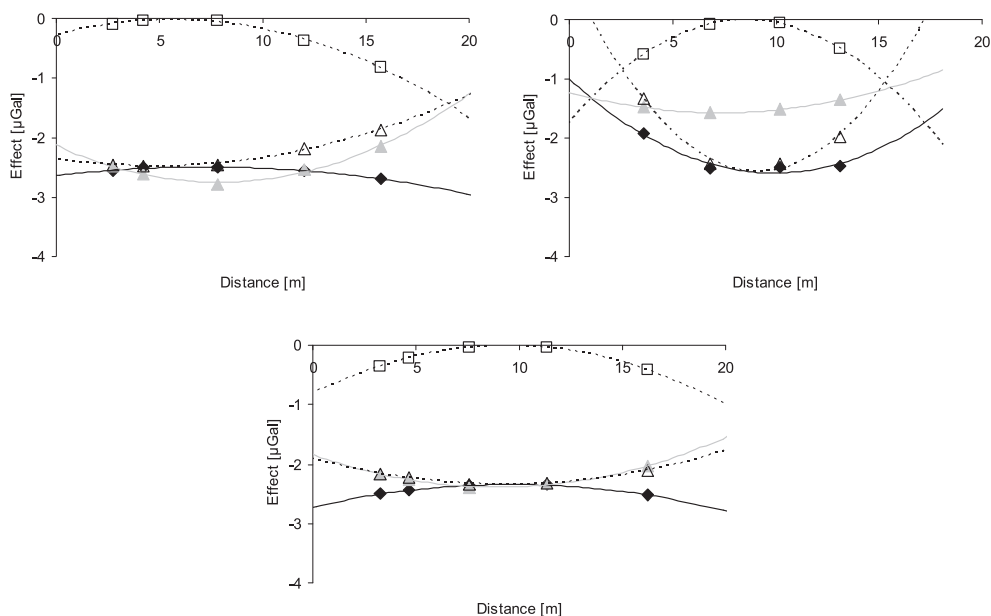


Fig. 6. The evaluated total effect (black diamonds and solid lines, the equation (18)) on gravity measurement with FG5-215, FG5X-251 equipped with the original collimator and FG5X-251 with the new triplet collimator (Thorlabs TC25APC-633), respectively. Its contributions, the diffractive (open triangles, (17)) and the divergence (open squares, (19)) terms are compared with the Monchalin's approximation (gray symbols and lines) calculated from the local beam widths. The values extrapolated to the zero distance were used for correcting measurements of gravimeters.

The estimated effects for individual gravimeters were obtained from Fig. 6 by extrapolating the total effects to the zero distance. The effects are  $(-2.64 \pm 0.03) \mu\text{Gal}$ ,  $(-1.01 \pm 0.42) \mu\text{Gal}$  and  $(-2.72 \pm 0.02) \mu\text{Gal}$  for FG5-215, FG5X-251 with the original collimator and FG5X251 with the new triplet collimator, respectively. The associated standard error estimates represent contributions from fitting and extrapolation errors, only. As it can be seen from Fig. 6 and error estimates, the estimated effect for a lower quality beam from the original collimator of the

FG5X-251 is quite uncertain due to a high fit/extrapolation error that even tends to an unreasonable value of  $+0.72 \mu\text{Gal}$  obtained for the diffractive term. This discrepancy can be caused by the fact that the beam at the collimator output is composed of more beams (probably from parasitic reflections) with different parameters and then their interference modifies the beam profile (as shown in Fig. 4) while the pure-mode beam profile only spreads with a distance. Therefore, in this case (FG5X-251 with the original collimator), the total effect will not be represented by the extrapolated value of  $-1.01 \mu\text{Gal}$ , that even does not reach the effect of diffraction-limited beam with corresponding beam width. The average total effect and its standard error of mean from all examined distances reaching value of  $(-2.35 \pm 0.12) \mu\text{Gal}$  will be used instead.

### 3.5. Other parameters of interfering beams

The camera beam profiling method further enables to determine (as secondary results) additional parameters of the interfering beams that can be used for correcting  $g$ -values or for improving the evaluation of measurement uncertainty.

To optimize the fringe signal, the two interfering beams are standardly aligned by translation and angular adjustment of the test beam relative to the reference beam. For a particular alignment, images of both beams were taken without camera movement at a particular distance. The evaluation of images showed that the centroids of reference and measuring beams from the interferometer output are distant by less than 20% of beam width. According to the equation 5 in [8], such a misalignment affects the difference of effective  $\delta k$  by less than 4% for the Gaussian beam (*i.e.* less than  $0.1 \mu\text{Gal}$  for gravimeters with a diffraction correction of about  $2 \mu\text{Gal}$ ). Since the obtained coordinates  $x$  and  $y$  match well the interfering fields  $E_1$  and  $E_2$  used in the calculations of the diffractive effect (including the centroid shift), the centroid correction from [8] should not be applied within our profiling method. Nevertheless, the overlap of the collimated beams in the position of the camera is different from the overlap in the detector plane that is behind the focusing lens in gravimeters. It means that in the detector plane, the overlap of beams also depends on the parallelity of beams. Therefore, the overlapping effect obtained from the camera images might be underestimated. The angular alignment of beams (parallelity of the reference and measuring beams from the interferometer output) was quantified from centroid differences at different distances and it was found to be better than  $10 \mu\text{rad}$  for  $M^2 = 1.2$  quality beams. However, it could reach  $20 \mu\text{rad}$  for a low quality beam given by the original collimator. Nevertheless, a beam shear does not affect  $g$  measurements directly as in the case of verticality misalignment [4] given by the angle between the effective wave vector (spatial frequency) of the measuring beam and the vertical direction of displacement to be measured. In the detector, the optical frequency beat between interferometer arms of a counting interferometer is not influenced by the geometry in front of this detector. The angular misalignment of beams only influences spatial frequencies and the contrast of the interferometer signal. We have to point out that such a conclusion does not correspond with (5) in [8], where the mutual angular misalignment of beams directly influences the interferometer fringe counting. We found that the distances between the centroids of collimated reference and measuring beams in gravimeters are often above  $0.1 \text{ mm}$  that is caused by the accuracy of alignment. Focusing such beams to the detector by a lens with a focal distance of about  $40 \text{ mm}$  produces an angle between the beam axes, which, according to [8], could affect the results of measurements in the order of up to hundreds of  $\mu\text{Gal}$ . However, such a huge effect has never been observed by absolute gravimeters and thus the angular correction from [8] should not be applied.

#### 4. Comparison of results

The gravity effects that correspond to the effective wavenumbers determined by the methods discussed in Sections 2 and 3 are given in Table 2. These results are compared with the Monchalin’s approach using a measured beam waist (instead of a beam width at a particular distance). We can see that the results of individual methods are quite ambiguous as the method based on the Monchalin’s approach has the largest effect for FG5-215, the diaphragm method has the largest effect for FG5X-251 with the original collimator and the camera method has the largest effect for FG5X-251 with the new collimator. Main contributions to the uncertainty budget for all three methods are caused by systematic effects that can be hardly estimated. Generally, the camera method should be the most accurate, but for beams with a really low quality we also found a problem caused by the uncertain extrapolation. Thus, we recommend that the average of all three methods should be used as the representative value for correcting gravimetric measurements. These average corrections are almost identical,  $2.4 \mu\text{Gal}$  for FG5-215 and about  $2.2 \mu\text{Gal}$  for FG5X-251. Further, we can see that the effects estimated with the three methods are within roughly  $1 \mu\text{Gal}$  for a particular gravimeter. Therefore, we suppose that the expanded uncertainty of the average effects will not be worse than  $0.9 \mu\text{Gal}$ . Generally, we can say that all the estimates of a so called diffraction correction (according to [4, 5]) for FG5(X) gravimeters discussed within this paper, are certainly larger than the value of  $1.2 \mu\text{Gal}$  that is usually applied to FG5(X) gravimeters with the original fibre collimator, according to the results from [4]. Moreover, the diaphragm method clearly shows that the effect (slopes) for the original collimator of FG5X-251 is larger than that for the new collimator. Note, that the effect with the new collimator cannot be as small as  $-1.2 \mu\text{Gal}$ , because the beam width and waist of a nearly Gaussian (*i.e.* diffraction-limited) beam measured for the new collimator is too small. In order to verify the difference between collimators, we also carried out  $g$  measurements with repeated replacements of collimators (five times) in the FG5X gravimeter. The obtained difference between the original and the new collimator was found to be  $-0.13 \mu\text{Gal}$  with the standard error of mean of  $0.55 \mu\text{Gal}$  (that also includes repeatability of beam adjustments), showing that the difference between the collimators is smaller and probably with the opposite sign than could be assumed from the beam widths only. Concluding, the usual correction of  $1.2 \mu\text{Gal}$  is probably underestimated and a larger correction should be applied. Nevertheless, it is worth considering to determine the effective wavenumbers for all particular gravimeters, since the beam width of FG5(X) gravimeters with the fibre optics looks different already at first glance. Further, as shown by the camera method, the beam quality plays an important role, too.

Table 2. Effects of the effective wavenumber on measurements with gravimeters in  $\mu\text{Gal}$  according to the following methods: 1) Monchalin’s approach in [1] for measured beam waists of the measuring beam; the results correspond approximately to the knife-edge method [4] carried out at the position of beam waist; 2) the method with an iris diaphragm (Section 2 and 3) the method with a profiling camera (Section 3) where the diffractive term and the total effect are tabulated. Further, the average values from three methods (using the total effect of camera method) are shown.

gravimeter	Monchalin	Iris method	Camera method		Average
	(12) in [1]	from (4)	diffractive, (17)	total effect, (18)	
FG5-215	-2.72	-1.71	-2.36	-2.64	-2.36
FG5X-251 orig. collimator	-1.54	-2.51	-2.04	-2.35	-2.13
FG5X-251 new collimator	-2.34	-1.78	-1.90	-2.72	-2.28

## 5. Conclusions

Two methods for determination of the effective wavenumber in absolute gravimeters have been presented.

The method based on the iris diaphragm is easy to apply if the photodetector of a gravimeter is equipped with mounting threads. The method works well for good quality Gaussian beams and the diffraction correction is evaluated directly from  $g$ -values measured *in situ*. During the evaluation, only the iris diaphragm opening is altered between the measurements and thus this method minimizes the influence of other effects. Nevertheless, we have to note that the zero-crossing detection system of a gravimeter must be independent of the fringe size, since the fringes are significantly changed by opening/closing the diaphragm. As shown in [13] the original system of FG5(X) does not meet such requirements but, for example, a new system discussed in [13] might be used [14] for any FG5(X). If both systems are running in parallel and the diaphragm is mounted on the new system, the effective wavenumber correction can be evaluated well from 300 free-falls. Therefore, the method can be easily repeated and the laboratory conditions are not required. In the case of low quality beams, as detected for FG5X-251, we would recommend to replace the original collimator by *e.g.* Thorlabs TC25APC-633 that is helpful also due to its pre-aligned and fixed collimation.

The camera method is time-consuming, difficult to be applied outside the laboratory and requires a careful and accurate evaluation of beam images. However, the method itself is more general and can be also applied to lower quality beams. Nevertheless, the beam quality can be simply improved by using better optical elements.

Comparing the results of both methods, we should also note that we expected better agreement of the two methods. Larger effects can be expected from the camera method, because the beam quality is taken into account. However, this assumption is not valid for lower quality beams, as it can be seen from Table 2. Further investigations are planned on this topic.

## Acknowledgements

The project “Advanced processing of absolute gravity measurements and investigation of systematic instrumental effects” is funded by the Czech Science Foundation (GA ČR) as grant no. 16-14105S and it is also supported by ČMI and VÚGTK.

## References

- [1] Monchalin, J.P., Kelly, M.J., Thomas, J.E., Kurmit, N.A., Szöke, A., Zernike, F., Lee, P.H., Javan, A. (1981). Accurate laser wavelength measurement with a precision two-beam scanning Michelson interferometer. *Appl Opt.*, 20(5), 736–57.
- [2] Sasso, C.P., Massa, E., and Mana, G. (2016). Diffraction effects in length measurements by laser interferometry. *Optics Express*, 24(6), 6522–6531.
- [3] Niebauer, T.M., Sasagawa, G.S., Faller, J.E., Hilt, R., Klotting, F. (1995). A new generation of absolute gravimeters. *Metrologia*, 32, 159–180.
- [4] vanWestrum, D., Niebauer, T.M. (2003). The diffraction correction for absolute gravimeters. *Metrologia*, 40, 258–263.
- [5] Robertsson, L. (2007). On the diffraction correction in absolute gravimetry. *Metrologia*, 44, 35–39.

- [6] Jiang, Z., *et al.* (2012). The 8th International Comparison of Absolute Gravimeters 2009: the first Key Comparison (CCM.G-K1) in the field of absolute gravimetry. *Metrologia*, 49, 666–684.
- [7] Trimeche, A., Langlois, M., Merlet, S., Pereira Dos Santos, F. (2017). Active Control of Laser Wavefronts in Atom Interferometers. *Phys. Rev. Applied*, 7, 034016.
- [8] Mana, G., Massa, E., Sasso, C., Andreas, B., Kuettgens, U. (2017). A new analysis for diffraction correction in optical interferometry. *Metrologia*, 54, 559–565.
- [9] Azuma, Y., *et al.* (2015). Improved measurement results for the Avogadro constant using a <sup>28</sup>Si-enriched crystal. *Metrologia*, 52, 360–375.
- [10] Fujii, K., Bettin, H., Becker, P., Massa, E., Rienitz, O., Pramann, A., Nicolaus, A., Kuramoto, N., Busch, I., Borys, M. (2016). Realization of the kilogram by the XRCD method. *Metrologia*, 53, A19–A45.
- [11] Zhan, Q. (2004). Second-order tilted wave interpretation of the Gouy phase shift under high numerical aperture uniform illumination. *Opt. Com.*, 242, 351–360.
- [12] Andreas, B., Fujii, K., Kuramoto, N., Mana, G. (2012). The uncertainty of the phase-correction in sphere-diameter measurements. *Metrologia*, 49, 479–486.
- [13] Křen, P., Pálinkáš, V., Mašika, P. (2016). On the effect of distortion and dispersion in fringe signal of the FG5 absolute gravimeters. *Metrologia*, 53, 27–40.
- [14] Křen, P., Pálinkáš, V., Mašika P., Val'ko, M. (2018). FFT swept filtering, a bias-free method for processing fringe signals in absolute gravimeters. Accepted in *Journal of Geodesy*.
- [15] Mana, G., Massa, E., Rovera, A. (2001). Accuracy of laser beam center and width calculations. *Appl Opt.*, 40(9), 1378–1385.